Pergamon

Oral Oncol, Eur J Cancer, Vol. 32B, No. 2, pp. 97–105, 1996

Printed in Great Britain
0964–1955/96 $15.00 + 0.00

0964–1955(95)00080–1

Growth Pattern of Experimental Squamous Cell Carcinoma in Rat Submandibular Glands—An Immunohistochemical Evaluation

S. Sumitomo, K. Hashimura and M. Mori

Department of Oral and Maxillofacial Surgery, Asahi University School of Dentistry, Hozumi, Motosu-gun, Gifu 501-02, Japan

Histopathological and immunohistochemical studies during carcinogenesis in rat submandibular glands (SMGs) using a carcinogen (9,10-dimethyl-1,2-benzanthracene: DMBA) were evaluated. For carcinogenesis, the carcinogen-containing sponge was surgically inserted into the gland. Histopathological features during carcinogenesis were as follows; dilatation of ductal segments, the presence of duct-like structures and cystic lesion around the sponge were observed within 3 weeks of the experiment, squamous metaplasia in duct-like structures and lining epithelium of the cystic structures around the sponge were observed at 4–6 weeks of the experiment, and finally well differentiated squamous cell carcinomas (SCCs) were observed after 8 weeks of the experiment. The immunoreactivity of K8.12 keration (K8.12), S-100 protein (S-100), epidermal growth factor (EGF), laminin, and proliferating cell nuclear antigen (PCNA) were evaluated. In the normal SMG, EGF was confined to the granular cells and S-100 to the pillar cells of granular convoluted tubules (GCTs). K8.12 was found in striated (SD) and excretory duct (ED) cells and laminin showed linear staining of the basement membrane around the ducts, acini and blood vessels. PCNA-positive nuclei were rarely observed in the normal glandular parenchyma. During carcinogenesis, during the first stage, EGF in granular cells and S-100 in pillar cells of GCT segments disappeared, and cytokeration K8.12 was observed in duct-like structures and cystic epithelium around the DMBA sponge. PCNA-positive nuclei in the first stage were mainly confined to basal cells of morphologically altered ducts. During the second stage, squamous metaplastic cells showed an intense K8.12 reaction. During the third stage, the well differentiated SCC showed strong reaction for K8.12, and the linear staining for laminin staining had disappeared at the invading fronts. The PCNA index was nearly 40% in the tumour cell component. The stem cells or the progenitor cells during experimental carcinoma were most likely to be the ductal basal cells, and carcinogenesis was initiated with an increase of proliferating activity in small cell clusters surrounding a necrotic area, basal cells of dilated excretory ducts and duct-like structures. Thus, all ductal segments undergoing squamous metaplasia may participate in the genesis of neoplasia during experimental carcinogenesis. Copyright © 1996 Elsevier Science Ltd

Keywords: experimental carcinoma, submandibular glands, immunohistochemistry

Oral Oncol, Eur J Cancer, Vol. 32B, No. 2, pp. 97–105, 1996.

INTRODUCTION

Histogenic concepts on salivary gland tumours in humans have often been cited via the semipleuripotential bicellular reserve cell hypothesis [1, 2]. The hypothesis considers that specific reserve or basal cells of excretory and intercalated ducts are responsible for the replacement of all types of cells in normal salivary glands and are the sole cells for neoplastic transformation. However, evidence is lacking for specific reserve cells in salivary gland neoplastic lesions. Histopathological examination of salivary gland tumours does not reveal an early stage of carcinogenesis and the majority of tumours often show a diverse histomorphology and tumour cell differentiation. Experimentally induced carcinoma in the salivary gland of laboratory animals using chemical carcinogens has been extensively studied [3–12]. Histologically, most of the experimentally induced tumours are reported as squamous cell carcinoma (SCC) and fibrosarcoma, and adenoma or adenocarcinoma are rare or virtually non-existent in experimental

Correspondence to S. Sumitomo.
Received 15 June 1995; provisionally accepted 9 Aug. 1995; revised manuscript received 14 Nov. 1995.

models. Moreover, the submandibular glands (SMG) of rats and mice are different from human SMG. SMG of rodents are characterised by the presence of granular convoluted tubule (GCT) segments in the ductal system which are one of the most differentiated secretory components in SMG and consist of three types of cells, namely granular, pillar and transition cells [13–16]. These structural components can be more readily distinguished by immunohistochemical methods, where epidermal growth factor (EGF) is a marker for granular cells and S-100 for pillar and transition cells [16–18]. The present study attempts to elucidate the histomorphological and immunohistochemical features of these cells during experimental carcinogenesis.

The present study deals with experimentally induced SCC in rat submandibular glands using our method of surgical implantation of 9,10-dimethyl-1,2-benzanthracene (DMBA) containing sponge, which resulted in a high frequency of carcinogenic changes, and histopathologically all tumours were well differentiated SCC. DMBA is one of the most potent carcinogens, acting as both initiator and promoter for carcinogenesis and is sometimes used for salivary gland carcinogenesis by injection, and pellet or crystal implantation in previous papers [5–7, 11]. The present study describes immunohistochemical evaluation of K8.12 keratin (K8.12), rat EGF, S-100 protein (S-100), laminin and proliferating cell nuclear antigen (PCNA) in normal and carcinogen implanted glands during experimentally induced tumour development.

MATERIALS AND METHODS

Experimental carcinogenesis of submandibular glands in rats

A total of 112 male and female Sprague-Dawley rats, 8 weeks old and weighing 180–200 g were obtained from Chubu Kagakusizai (Japan) at least 2 weeks before the experiment and maintained under standard laboratory conditions with access to food and water *ad libitum*. Under pentobarbital sodium anaesthesia, the right SMG was exposed by surgical procedure. A sponge pellet (2 × 2 mm Tokuso, Japan) designed for composite-resin restoration of the tooth was used as the carrier of the carcinogen. The sponge containing 1% DMBA (Sigma, U.S.A.)/olive oil solution was implanted into the glandular tissue of the right SMG. The incision was closed with silk threads. Sixteen rats (8 females and 8 males) were killed at 1, 2, 3, 4, 6, 8, 12 weeks after the DMBA/sponge implantation. The SMGs were fixed in 10% buffered formalin solution for 24 h, embedded in paraffin and 4 μm sections were made for histopathological and immunohistochemical studies.

The same method of sponge implantation without containing DMBA was carried out as a control. Two control rats of both sexes were killed at 2, 6, and 12 weeks after implantation. There was no tumour genesis found in control rats. Slight imflammatory cell infiltration was found limited around the sponge implanted section in 2 week specimens and histologically normal findings were observed in 6 and 12 weeks specimens.

Immunohistochemical methods

For immunohistochemical study, the sections were deparaffinised and rehydrated in a graded alcohol series and treated with methanol containing 0.05% hydrogen peroxide for 30 min to block endogenous peroxidase activity. The sections were then treated with normal rabbit serum (1:20) for 30 min to block non-specific background staining. This was followed by incubation with monoclonal antibody (Table 1) for 1 h at room temperature. After rinsing three times for 5 min each in phosphate buffered saline (PBS), the second antibody, biotinylised anti-mouse IgG (1:200 Dako, Denmark) was used and washed with PBS. This was followed by the peroxidase conjugated avidine–biotin complex (1:500 Dako, Denmark) reaction and peroxidase activity was visualised by 0.03% 3.3-diaminobenzidine tetrahydrochloride (Dojin, Japan) and 0.05% hydrogen peroxide. In the case of laminin, the tissue sections were subjected to trypsin pretreatment (0.01% trypsin/PBS solution, pH 7.6, 5 min).

Table 1. List of primary antibodies

Antibody	Dilution	Source
K8.12	1/40	Biomarker, Israel
S-100 α	1/100	JIMRO, Japan
r-EGF	1/200	Ohtuka, Japan
Laminin	1/100	Chemicon, U.K.
PCNA	1/20	DAKO, Denmark

The extent of PCNA positivity was evaluated by determining the positively stained nuclei present in at least 500 cells in each structure of the specimen using a computer associated semi-automatic quantitative analyser (Magiscan 2A, Joyce-Level, U.K.).

RESULTS

Normal submandibular glands of the rat

SMGs of matured rats showed well developed GCTs in males which were less developed in the female and consisted of terminal acinar cells, intercalated ducts, GCTs, striated ducts and excretory ducts (Fig. 1A). GCTs had granular, pillar, and transition cells. Immunohistochemically, EGF was concentrated in granular cells (Fig. 1B), and S-100 in pillar and transition cells of GCT segment and striated duct cells (Fig. 1C). K8.12 showed conspicuous staining in excretory and striated ducts on the luminal side and no reaction product in GCT and acinar cells (Fig. 1D). Laminin was seen on the basement membrane of glandular structures and blood vessels. PCNA-positive nuclei were rare and almost no mitotic figures were observed in all glandular parenchymal cells (Fig. 2).

Histopathological and immunohistochemical findings during carcinogenesis

The process of carcinogenesis was as follows; necrotic and degenerative changes were first observed in glandular cells, which corresponded to an initiation event following carcinogen application, after which formation and squamous metaplasia of cyst-like structures around the carcinogen-containing sponge and duct-like structures occurred and finally SCCs were induced and invaded surrounding tissues.

Changes within 3 weeks of experiment

Histopathologically, three concentric circular patterns centering around the DMBA/sponge were observed (Fig. 3A). The inner layer showed necrosis with rough and oedematous connective tissue, the middle layer showed inflammation, and the outer layer had histologically normal intact gland. In the

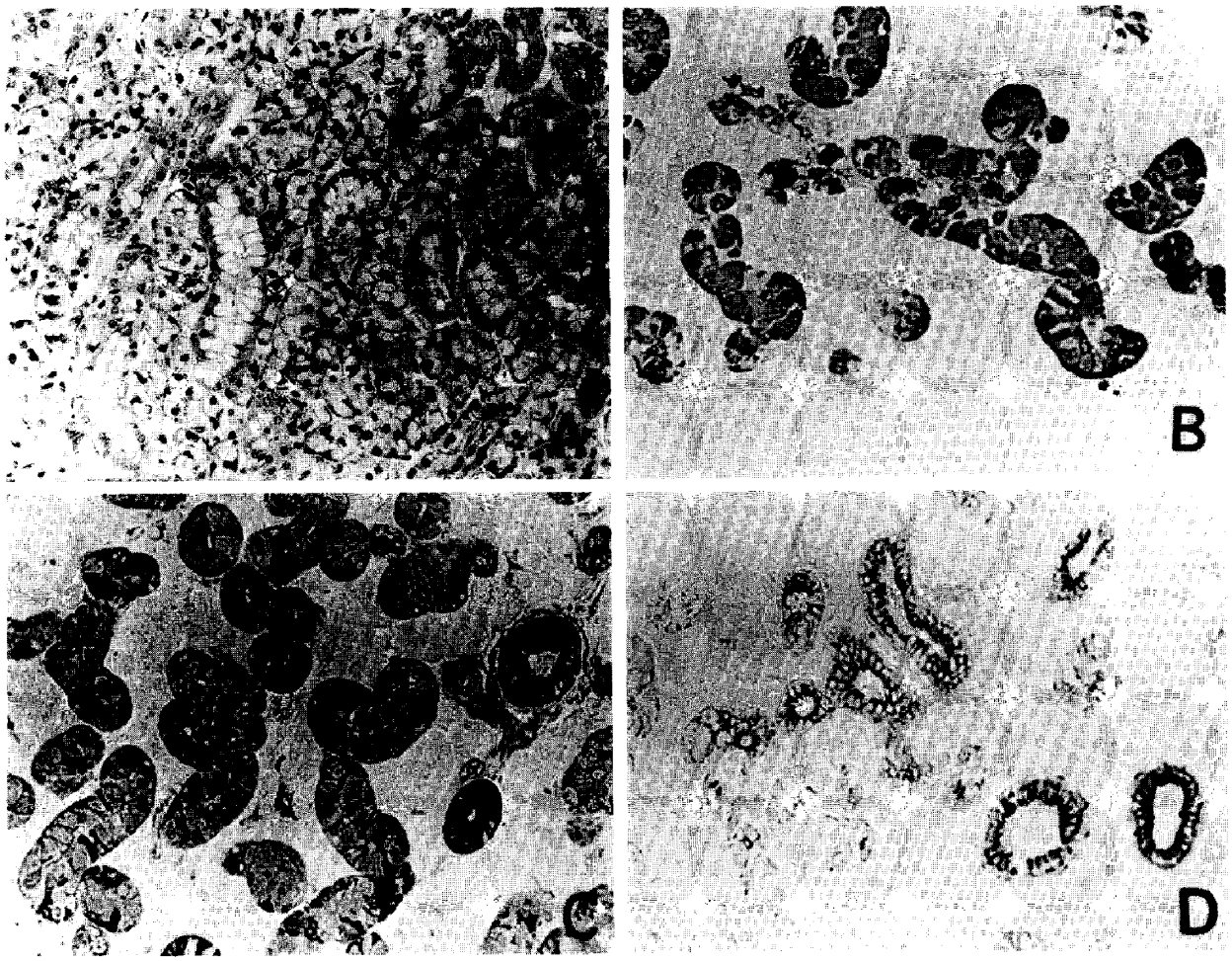

Fig. 1. Normal male rat SMG (×100). (A) HE staining; (B) EGF staining. Granular cells in GCT segments showed strong staining; (C) S-100 staining. Pillar and transition cells in GCT segments showed strong staining and granular cells in GCT segments and intercalated duct cells showed weak staining; (D) K8.12 staining. Striated and excretory duct cells showed positive staining.

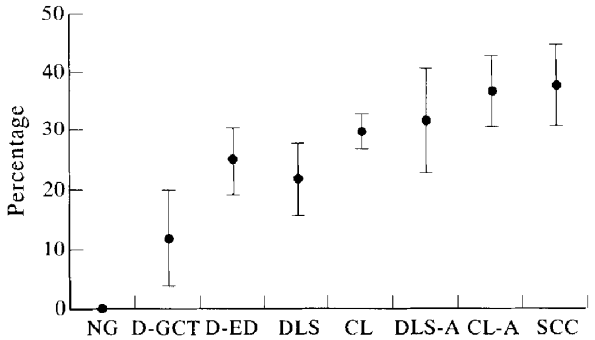

Fig. 2. Staining index of PCNA during carcinogenesis in rat SMG. NG, normal submandibular gland; D-GCT, dilated granular convoluted tubules; D-ED, dilated excretory duct; DLS, duct-like structure; CL, cystic lesion; DLS-A, DLS with cellular atypia; CL-A, CL with cellular atypia; SCC, squamous cell carcinoma.

innermost necrotic area surrounding carcinogen-containing sponge, most of the glandular cells had disappeared, numerous small cell clusters and excretory ducts remained. Large excretory ducts in this area showed dilatation of their lumen and there were numerous instances of squamous metaplasia of ductal cells (Fig. 3B). The tissues were inflamed around the necrotic mass, where most acinar cells had disappeared and ductal segments were dilated. Owing to the degranulation of granular cells, it was difficult to identify granular, pillar and transition cells in the GCT segment. However, in the 2 week specimen, duct-like structures had developed from GCT segments (Fig. 3E).

Immunohistochemical observations within 3 weeks of experiment. Changes were observed in the immunostaining for EGF, S-100, K8.12, and PCNA in the tissue specimen. The inner zone, containing squamous metaplastic cells in the large excretory duct and small clusters of remaining cells had an intense immunoreaction for K8.12 (Fig. 3C). PCNA staining was confined to the nuclei of basally located cells of the dilated and squamous metaplastic excretory duct (staining index (SI) = 25%) and numerous nuclei in the cell clusters (Fig. 3D). In inflamed areas, EGF immunoreactivity was decreased or disappeared in degranulated granular cells (Fig. 3F) and S-100 staining was decreased in pillar and transition cells. The conspicuous staining for K8.12 was seen in altered GCT

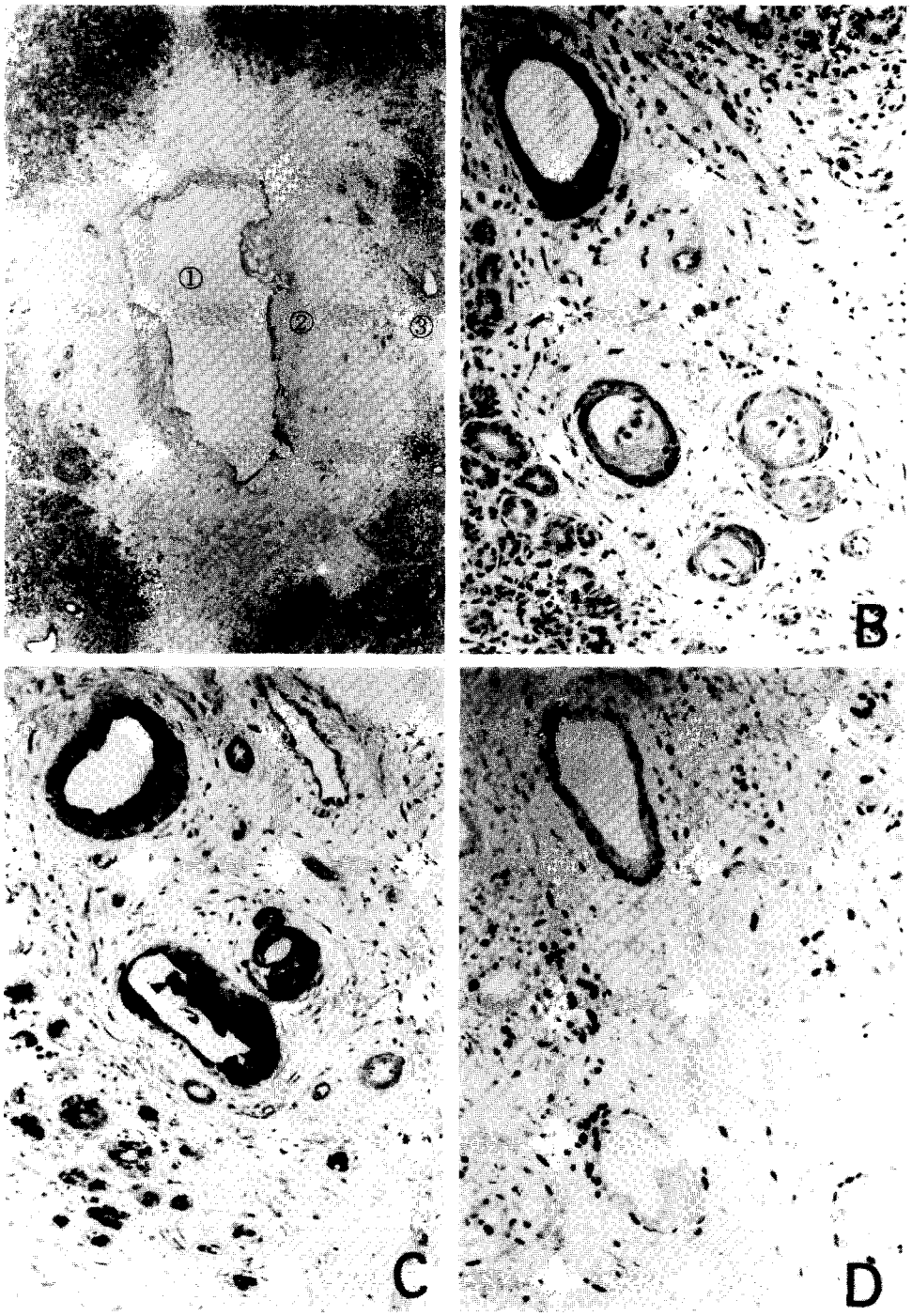

Fig. 3(A)–(D).

segments and duct-like structures, with few cells showing intense staining (Fig. 3G). PCNA staining in this area was found in the nuclei of the cells in altered GCT segments (SI = 12%) and duct-like structures (SI = 22%) as well as in the nuclei of inflammatory cells (Fig. 3D). Mitotic figures were also found in the same segments as PCNA-positive cells but mitotic figures were usually negative for PCNA staining and their intensity was very low. Laminin immunostaining was found in the basement membrane as a continuous band surrounding duct-like structures and capillary blood vessels (Fig. 3H).

4–6 *weeks of experiment*

The central necrotic mass was separated by a thin cystic lining. This cystic wall consisted of ortho-keratinised squamous epithelium, which had an increased thickness and advanced squamous metaplasia depending on the duration of the lesion. Some parts of the cystic epithelium showed proliferation both at the luminal side as a papillary projection and the basal side as epithelial down-growth. Cellular atypia was rare in 4 week specimens (Fig. 4A, B). Cystic epithelium had extensive exophytic and endophytic growths, and in some instances dysplasia or early SCC were observed in 6 week

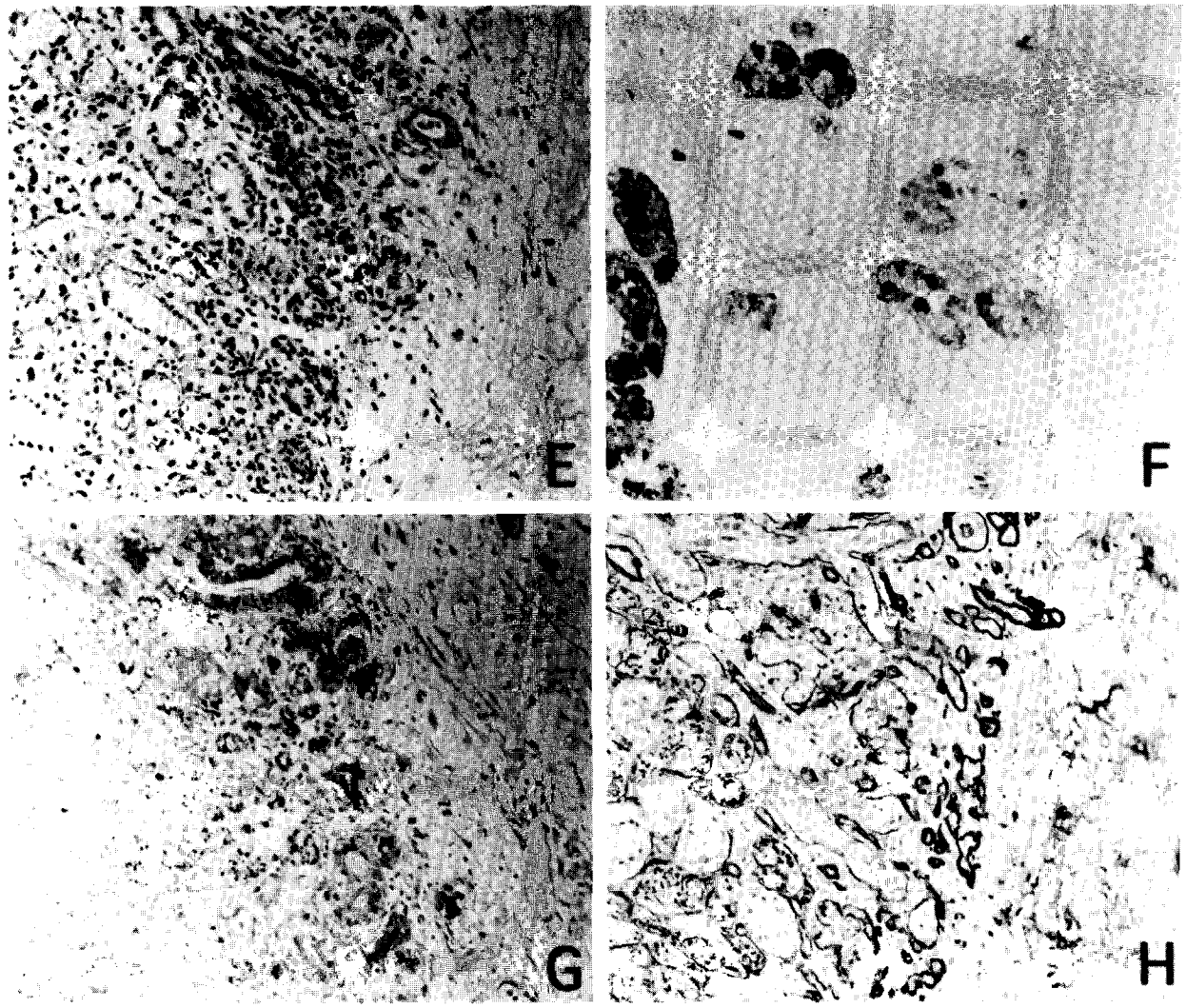

Fig. 3(E)–(H).

Fig. 3. Two weeks after DMBA/sponge implantation (A) × 10; (B)–(H) × 100. (A) HE staining. Three zonal pattern centering around DMBA/sponge-implanted cavity can be observed. DMBA/sponge implanted cavity ① is surrounded by necrotic and oedematous area ②, inflammatory zone ③, and almost normal glandular tissue; (B) HE staining. Large excretory ducts with papillary hyperplasia were found in the inflammatory area; (C) K8.12 staining. Luminal layer of affected large excretory ducts showed strongest staining; (D) PCNA staining. PCNA-positive nuclei were observed in the basal cells of affected excretory ducts, duct-like structures, and inflammatory cells; (E) HE staining. Border zone between the inflammatory area and almost normal glandular tissue. Duct-like structures and degranulated GCT segments were found in inflamed areas. Acinar cells showed degenerative change; (F) EGF staining. Granular cells in normal GCT segments showed strong staining, although, duct-like structures and degranulated GCT segments showed weak or almost negative staining and there were few strong positive cells remaining; (G) K8.12 staining. Normal acini and GCT segments showed negative reaction. Duct-like structures and degranulated GCT segments showed weak to moderate staining and showed few strongly stained cells; (H) Laminin staining. Laminin staining was found continuously in the basement membrane of acinar compartments, GCTs, duct-like structures and capillary blood vessels.

specimens. Beneath the cyst lining, squamous epithelia showed connective tissue with abundant capillary blood vessels and duct-like structures with or without squamous metaplasia were also found in this area. The outer zone of surrounding connective tissue had adjacent lobules of SMG with a mixture of normal and altered glandular structures. The alteration in the glandular parenchyma was characterised by the disappearance of acinar cells, loss of secretory granules in the GCT segment and the formation of duct-like structures.

Immunohistochemical changes were dependent on histological changes; immunoreactivity for EGF and S-100 had decreased in degenerated structures while K8.12 staining was enhanced in squamous metaplastic cells the cystic structure showed a marked K8.12 staining except for the basal layer (Fig. 3C) and an increased index of PCNA staining in basal cell nuclei (SI = 30%) (Figs 2, 3D). Dilated and squamous metaplastic excretory ducts and duct-like structures showed similar immunostaining patterns as in the cystic epithelium with intense K8.12 staining in the luminal areas and PCNA staining in the basal cell nuclei (SI = 37%). PCNA-positive nuclei were also found in duct-like structures and inflamed connective tissue. Mitotic figures were also found in the basal

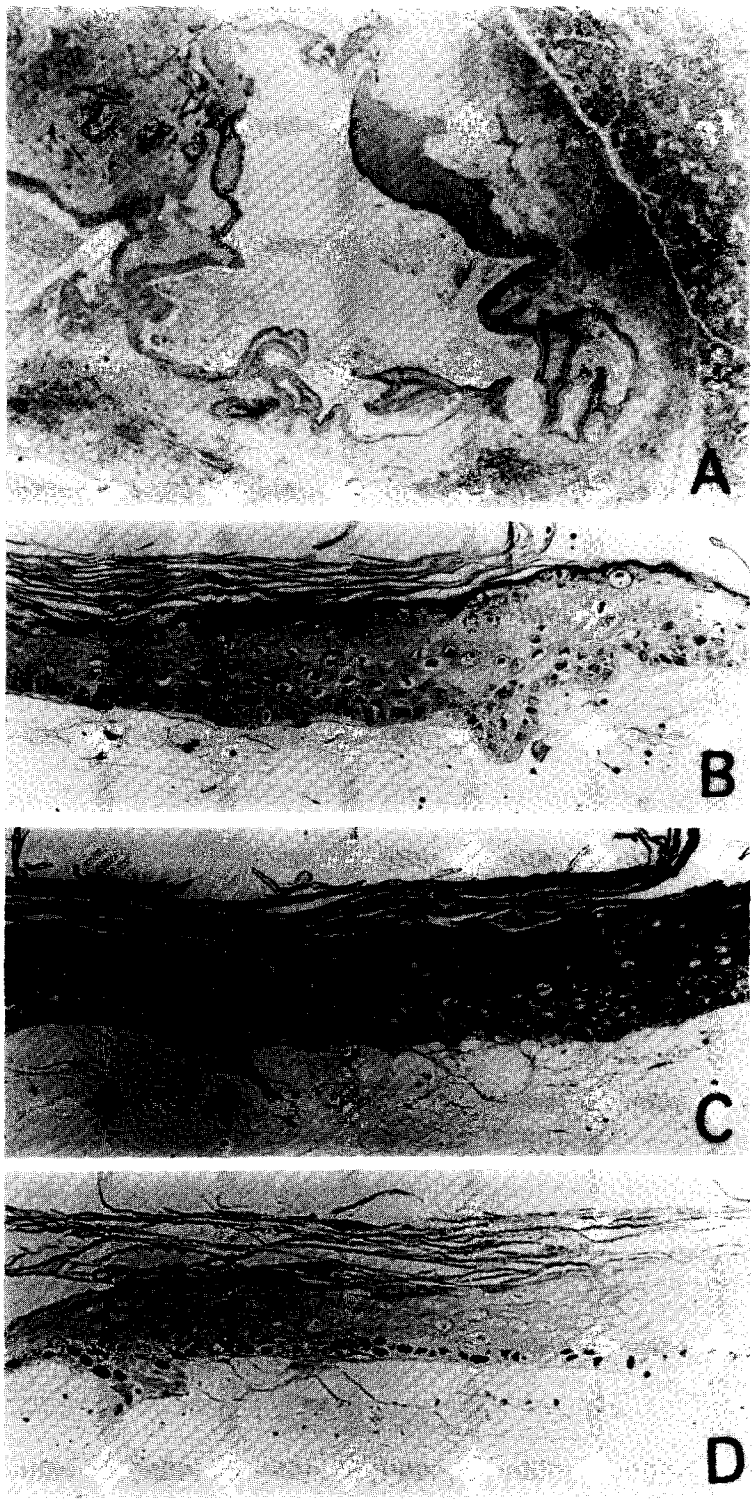

Fig. 4. Four weeks after DMBA/sponge implantation. (A) ×10; (B)–(D) ×200. (A) HE staining. Well-keratinised squamous epithelial cell containing cyst lining was formed around the DMBA/sponge. Inflamed connective tissue, including duct-like structures with or without keratinisation, were observed surrounding cystic epithelium; (B) HE staining. Cyst-lining epithelium showed a well-keratinised squamous epithelium and partial basal cell hyperplasia was observed. Cellular atypia as pyknotic nuclei and dyskeratosis were sometimes observed; (C) K8.12 staining. Spinous, granular and keratinised layers showed strong staining and basal and the parabasal layer showed weak staining; (D) PCNA staining. PCNA positive nuclei were limited in the basal cell layer.

layer of cyst-like and duct-like structures and the frequency was increased. Laminin staining showed a continuous positive band on the basement membrane of cyst-like and duct-like structures. Furthermore, many capillary blood vessels adjacent to the cystic and duct-like structures showed intense laminin staining on their basement membrane.

After 8 weeks experiment

Cystic epithelium surrounding the carcinogen-containing sponge and squamous metaplastic duct-like structures showed extensive growth and transformed into a premalignant and carcinomatous lesion. Hyperkeratosis of the cystic and duct-like squamous epithelium with cellular atypia and basal cell down-growth were frequently seen as a premalignant sign. Induced carcinoma was histologically classified into well and moderately keratinised SCC. Small nuclear fragments were frequently observed in the hyperkeratinised area. Hyperchromatic nuclei and dyskeratosis were frequently seen in these lesions. Large neoplastic masses, composed of papillary configuration and invading a small nest of SCC showing well to moderately differentiated SCC, were obtained after 12 weeks of DMBA/sponge implantation (Fig. 5A, E). Tumour foci showed both invasive and expansive growth although no metastases were observed in regional lymph nodes and other organs.

Immunohistochemically, K8.12 showed moderate to intense staining in the upper layer and weak staining in the basal and para-basal layer of tumour epithelium (Fig. 5B). PCNA-positive nuclei were distributed in the basal and parabasal cells in the expansive growth area (Fig. 5C), as in the invading-growth front (Fig. 5F) and the staining index rose to the highest level (SI = 38%, Fig. 2). Mitotic figures were sometimes found in the basal and parabasal area of SCC foci. Laminin staining at the interface between tumour nests and stroma were varied. It was found as a continuous band at the basement membrane surrounding the tumour focus in the expanding growth area (Fig. 3D), but was absent in invading fronts of SCC (Fig. 3G) and a combination of these two were sometimes seen in the same tumour focus. The basement membrane of capillary blood vessels situated in the peripheral stromal tissue showed strong staining for laminin (Fig. 3D, G).

DISCUSSION

In order to explore precursor or stem cells of salivary gland tumours, experimental tumours of salivary glands have been described by different methods using different carcinogens [3–12]. Carcinogenesis in salivary glands using carcinogens accompanying other reagents and factors have been reported to accelerate or inhibit tumour induction [19–22]. Tumour induction has been reported in 55–80% of experimental animals and histopathologically, epidermoid carcinoma and fibrosarcoma are the common lesions in earlier studies. Two types of methods: injection of carcinogen/oil solution [4, 7, 11]; and surgical insertion of carcinogen crystal [3] or pellet [5] were usually used in the previous experimental mode. The injection method is convenient but as the carcinogen is sprinkled in the glands and sometimes in the surrounding tissue during injection, it is difficult to identify the exact site of application. Carcinogen crystal implantation is a good way to apply a uniform dose at the same position, although crystallisation of the carcinogenic agent is not so easy. Carcinogen-containing sponge, as used in the present experiment, may be a better technique than injection and crystal implantation as 100% induction of keratinised squamous cell carcinoma was obtained within a relatively short duration (12 weeks).

Immunohistochemical markers in the present studies were based on earlier findings that: (1) EGF is confined to the granular cells in GCT segment as a secretory peptide [13, 16, 17]; (2) S-100, a calcium-binding protein, is located specifically in pillar and transition cells in the GCT segment and may influence secretion [18]; (3) K8.12 that reacts with cytokeratins 13 and 16, stains specifically squamous epithelium and SCCs (data sheet). K8.12 staining in rat SMGs has been found in striated and excretory ducts but not in GCT and acinar cells, and enhanced in ductal segments following duct obstruction [23]; (4) laminin is present in the basement membrane and is a useful marker for tumour invasion [24]; (5) PCNA is a co-enzyme of DNA polymerase-δ and a suitable marker for cellular proliferation activity [25, 26]. These markers were employed for immunohistochemical alterations during carcinogenesis in the salivary glands.

In the initial stage of carcinogenesis, the remaining cell clusters in the necrotic area surrounding DMBA/sponge showed a high potential for proliferation and expression of K8.12 keratin. These cells may have been derived from all ductal segments and transformed into keratinised SCC via cyst-like structure surrounding the DMBA/sponge. DMBA/sponge was covered by squamous epithelial lining within 4 weeks of the experiment. The epithelium may be formed either as an attempt to localise the carcinogen or may also be influenced by EGF, which is secreted from granular cells of GCT. At 6 weeks of the experiment, the K8.12 staining pattern in the cyst-like epithelium was similar to that of human oral leukoplakia and experimentally premalignant lesions in hamster cheek pouch. They stained strongly in the upper layer, negative in the basal layer, and diffusely in atypical epithelial cells. The growth pattern at this stage may not be invasive because the basement membrane, identified by laminin staining, was continuously present at the base of the cystic epithelium. After 10 or more weeks of the experiment, the growth pattern may change into an invasive one at a particular site, as, for example, where there was down-growth of cystic epithelium, laminin staining was not continuous. The PCNA index was increased to the maximum level (39.1%) in the invasive growth area. This index is higher than in the human oral leukoplakia, SCCs [27] and salivary gland tumours [28–30]. The changes in growth pattern and highly proliferating activity may have been induced by a continuous affect of the carcinogen.

Large excretory ducts such as interlobular ducts, seemed to be the only single histologically stable components remaining in the vicinity of the DMBA/sponge during the initial stage. This segment usually consists of two cell layers: the luminal and ductal basal cells. Ductal basal cells in the terminal segment seemed to be the origin of modified myoepithelium cells or neoplastic myoepithelial cells in pleomorphic adenoma in human salivary glands [31]. In the initial stage of our experiment, the proliferating activity of ductal basal cells was rapidly increased, ductal dilatation and papillary hyperplasia were found in affected excretory ducts, and further neoplastic changes in this component resembled epithelial carcinogenesis.

The GCT segments have been reported to be one of the origins of experimental carcinogenesis in rat and mice [5–7, 11, 12]. This may be because the formation of duct-like structures via degranulation of GCT is one of the dramatic changes in the initial stages of experimental carcinogenesis in SMG. The loss of EGF staining and enhanced K8.12 staining in the GCT segment were characteristic features. This suggests that the secretory cells in the GCT segment probably changed their nature and function as seen in squamous epithelial cells by the influence of carcinogen. Degranulation of granular cells

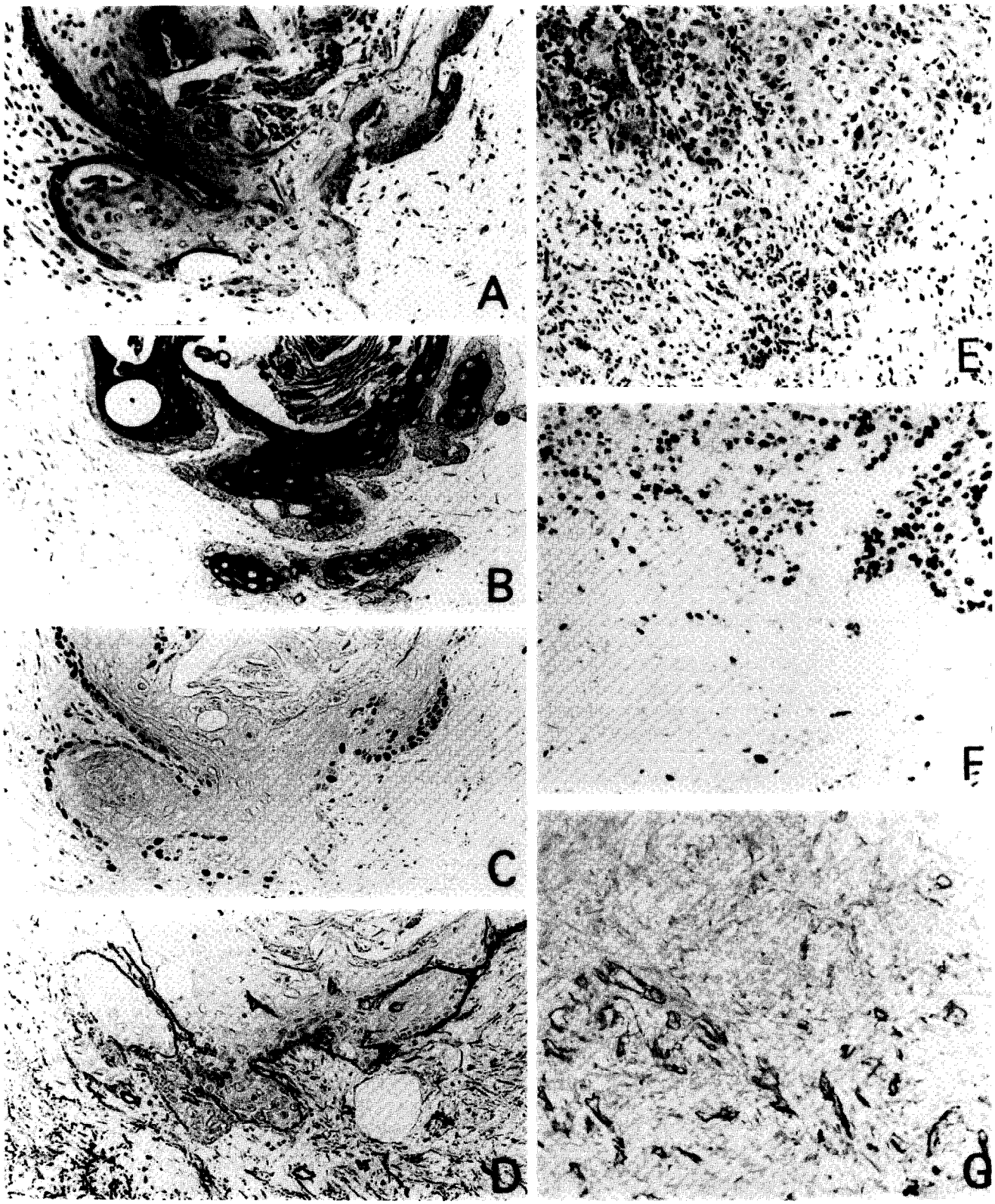

Fig. 5. Twelve weeks after DMBA/sponge implantation (×100). (A) HE staining. Well-keratinised squamous cell carcinoma formed a cystic structure surrounding the DMB/sponge. Invading growth patterns of basal aspects was partially observed in the cystic lesion. Nuclear fragmentation was frequently observed in the upper layer cells; (B) K8.12 staining. Upper layers except for fully keratinised cells showed strong staining and basal cells showed weak staining; (C) PCNA staining. PCNA-positive nuclei are limited in the basal cell layer; (D) Laminin staining. The continuous staining pattern of laminin on the basal layer shows fragment breaks at the invasive growth area; (E) HE staining. Squamous cell carcinoma with invading growth patterns were observed; (F) PCNA staining. PCNA-positive nuclei were scattered in the tumour focus; (G) Laminin staining. Laminin staining was negative surrounding the tumour foci and limited to the basement membrane of capillary blood vessels.

during carcinogenesis may be different from normal secretion. EGF secreted into saliva under the normal condition was influenced by an α-adrenergic effect [32], although in carcinogenesis, EGF may spread into SMG. This may be one of the reasons why the squamous cell carcinoma rapidly occurred in SMG. Normal GCT cells show a very low proliferation activity. However, the PCNA index in the altered GCT segment was increased with the formation of a duct-like structure. Degranulation, cellular proliferation and squamous metaplasia of the GCT segment have also been described after duct ligation, although in duct-ligated salivary glands, higher proliferating ratios in ductal segments were limited at an initial or early stage [33, 34].

From the present study, it is thought that all ductal cells in rat SMG may have high potential for proliferation and may transform to SCC via squamous metaplasia by topical application of carcinogen. PCNA-positive nuclei indicating the proliferation activity were limited to the basal cells of the altered ductal segment, and these ductal basal cells may correspond to reserve cells for the origin for salivary gland tumours.

The results of the present study support the conclusion that all ductal segments undergo squamous metaplasia and, therefore, may participate in the genesis of neoplasia during experimental carcinogenesis. However, the neoplastic lesions formed using this model are SCC arising in reactive metaplastic epithelium which has formed cyst-like structures around the sponge-implanting cavity. In the present study, we were unable to obtain the most complex and diverse histomorphology of neoplastic lesions which are routinely observed in salivary gland tumours. The factors resulting in a diverse histomorphology and tumour cell differentiation in salivary tissue are yet to be elucidated.

1. Eversole LR. Histogenic classification of salivary tumors. *Arch Pathol* 1971, **92**, 433–443.
2. Regezi JA, Batsakis JG. Histogenesis of salivary gland neoplasms. *Otolaryngol Clin North Am* 1977, **10**, 297–307.
3. Cataldo E, Shklar G. Chemical carcinogenesis in the hamster submaxillary gland. *J Dent Res* 1964, **43**, 568–579.
4. Cherry CP, Gluckmann A. The histogenesis of carcinomas and sarcoma induced in the salivary glands of rat. *Br J Cancer* 1965, **19**, 787–801.
5. Chaudhry AP, Liposky R, Jones J. Dose-response of submandibular gland to carcinogen pellets in rats and hamsters. *J Dent Res* 1966, **45**, 1548–1550.
6. Kim SK, Spencer HH, Weatherbee L, Nasjet CE. Changes in secretory cells during the early stages of experimental carcinogenesis in the rat submandibular gland. *Cancer Res* 1974, **34**, 2172–2183.
7. Mori M, Takai Y, Naito R, Hosaka M, Murase N. Immunohistochemical demonstration of epidermal growth factor and nerve growth factor in experimental carcinogenesis in the mouse submandibular gland. *Virchow Arch B* 1984, **45**, 431–441.
8. Shafer WG. Experimental salivary gland tumorigenesis. *J Dent Res* 1962, **41**, 117–124.
9. Standish SM. Early histologic changes in induced tumors of the submaxillary salivary glands of the rats. *Am J Path* 1957, **33**, 671–689.
10. Sugimura M, Kawakatsu K. Histochemical studies of enzymatic patterns during experimental carcinogenesis in the mouse partoid gland. *Archs Oral Biol* 1966, **11**, 1269–1291.
11. Takai Y, Murase N, Hosaka M, Kawamura K, Mori M. Immunohistochemical localization of kertin in experimental carcinoma of the mouse submandibular gland. *Virchow Arch B* 1984, **47**, 183–187.
12. Wigley CB, Carbonell AW. The target cell in the chemical induction of carcinomas in mouse submandibular gland. *Eur J Cancer* 1976, **12**, 737–741.
13. Gresik EW. The granular convoluted tubule (GCT) cell of rodent submandibular glands. *Microsc Res Tech* 1994, **27**, 1–24.
14. Hazen-Martin DJ, Simson JAV. Ultrastructure of the secretory response of male mouse submandibular gland granular tubules. *Anat Rec* 1986, **214**, 253–265.
15. Pinkstaff C. The cytology of salivary glands. *Int Rev Cytol* 1980, **63**, 141–261.
16. Mori M. *Histochemistry of the Salivary Glands*. Boca Raton, Florida, CRC Press, 1991.
17. Mori M, Takai Y, Kunikata M. Review: biological active peptide in the submandibular gland-role of the granular convoluted tubule. *Acta Histochem Cytochem* 1992, **25**, 325–341.
18. Hashimoto J, Jayasinghe N, Kunikata M, Takai Y, Mori M. Immunoreactivity of calmodulin, S-100 protein alpha and beta subunits in rat submandibular glands. *Arch Anat Cytol Path* 1992, **40**, 79–87.
19. Okada Y. Effect of isoproterenol on chemical carcinogenesis with DMBA in mouse salivary glands. *J Oral Pathol* 1979, **8**, 340–350.
20. Shklar G, Cataldo E. Effects of a chemical carcinogen on the submaxillary gland of albino rats treated with isoproterenol. *Cancer Res* 1966, **26**, 1319–1323.
21. Tubiner S, Shklar G, Cataldo E. The effect of cold stress on chemical carcinogenesis of rat salivary glands. *Oral Surg* 1970, **29**, 130–137.
22. Tatemoto Y, Takai Y, Saka M, Kumasa S, Iwai Y, Mori M. Immunohistochemical detection of epidermal growth factor in submandibular gland tumor mice administered testosterone. *Carcinogenesis* 1985, **6**, 1747–1753.
23. Jayasinghe N, Hashimoto J, Ogata K, Shrestha P, Takai Y, Mori M. Changes of calmodulin, S-100 protein αβ and keratin in duct-ligated salivary glands of rats—an immunohistochemical study. *Acta Histochem Cytochem* 1993, **26**, 555–562.
24. d'Ardenne AJ. Use of basement membrane markers in tumor diagnosis. *J Clin Pathol* 1989, **42**, 449–457.
25. Bravo R, Frank R, Blundell PA, MacDonald-Bravo H. Cyclin/PCNA is the auxillary protein of DNA polymerase-δ. *Nature* 1987, **309**, 515–517.
26. Prelich G, Tan CK, Kostura M, *et al.* Functional identity of proliferating cell nuclear antigen and a DNA polymerase-δ auxillary protein. *Nature* 1987, **326**, 517–520.
27. Tsuji T, Sasaki K, Kimura Y, Yamada K, Mori M, Shinozaki F. Measurement of proliferting cell nuclear antigen (PCNA) and its clinical application in oral cancers. *J Oral Maxillofac Surg* 1992, **21**, 369–372.
28. Ogawa I, Miyauchi M, Takata T, Vuhahula E, Ijuhin N, Nikai H. Proliferating activity of salivary gland pleomorphic adenomas and myoepitheliomas as evaluated by the proliferating cell nuclear antigen (PCNA) labeling index (LI). *J Oral Pathol Med* 1993, **22**, 447–450.
29. Yang L, Hashimura K, Qin C, Shrestha P, Sumitomo S, Mori M. Immunoreactivity of proliferating cell nuclear antigen in salivary gland tumours: an assessment of growth potential. *Virchow Arch A* 1993, **422**, 481–486.
30. Yang L, Liu B, Qin C, Hashimura K, Yamada T, Sumitomo S, Mori M. Comparison of proliferating cell nuclear antigen index in benign and malignant pleomorphic adenoma: using an antigen retrieval. *Oral Oncol* 1994, **30**, 56–60.
31. Mori M, Takai Y, Sumitomo S. Salivary gland tumors: a possible origin of modified myoepithelial cells is ductal basal cells. *Cancer J* 1992, **5**, 316–320.
32. Murphy RD, Watson AY, Metz J, Forssmann WG. The mouse submandibular gland: an exocrine organ for growth factor. *J Histochem Cytochem* 1980, **28**, 890–902.
33. Sumitomo S, Sumitomo KM, Hashimoto J, *et al.* Cell proliferation activity in duct-ligated submandibular gland. *Acta Histochem Cytochem* 1995, **28**, 1–9.
34. Walker NI, Gobe GC. Cell death and cell proliferation during atrophy of the rat parotid gland induced by duct obstruction. *J Pathol* 1987, **153**, 333–334.